



Supplement of

Aerosol–cloud interactions in cirrus clouds based on global-scale airborne observations and machine learning models

Derek Ngo et al.

Correspondence to: Minghui Diao (minghui.diao@sjsu.edu)

The copyright of individual parts of the supplement might differ from the article licence.

10 **Table S1.** Flight hours for each flight campaign in the cirrus temperature range, i.e., temperatures $\leq -40^{\circ}\text{C}$. The hours of measurements are separately shown for all-sky, clear-sky, and in-cloud conditions, as well as non-quiescent and vertically quiescent conditions. The non-quiescent conditions are defined as vertical velocity (w) $> 1 \text{ m s}^{-1}$ or $< -1 \text{ m s}^{-1}$ within ± 30 seconds surrounding each centre second. The rest is defined as vertically quiescent.

Field Campaign	Total flight hours at temperature (T) $\leq -40^{\circ}\text{C}$	Clear-sky conditions at T $\leq -40^{\circ}\text{C}$ (hours)	In-cloud conditions at T $\leq -40^{\circ}\text{C}$ (hours)	Non-quiescent clear sky (hours)	Vertically quiescent clear sky (hours)	Non-quiescent cirrus clouds (hours)	Vertically quiescent cirrus clouds (hours)
NSF HIPPO2-5	112.18	104.84	7.34	12.07	92.76	1.53	5.81
NSF START08	54.68	51.99	2.69	8.61	43.38	1.11	1.58
NASA SEAC ⁴ RS	14.77	10.07	4.70	2.92	7.15	3.27	1.43
NSF DC3	72.53	47.32	25.21	8.86	38.46	12.53	12.68
NASA DC3	29.68	15.74	13.94	3.90	11.84	8.38	5.56
NASA MACPEX	39.36	26.08	13.28	2.92	23.15	4.04	9.24
NSF CONTRAST	72.19	50.44	21.75	5.02	45.42	8.17	13.58
NASA ATREX-2014	126.69	91.95	34.74	2.63	89.32	1.77	32.97
NSF PREDICT	73.43	52.03	21.40	5.92	46.11	8.29	13.11
NASA POSIDON	40.93	27.71	13.22	1.66	26.05	1.52	11.70
NSF TORERO	53.89	51.62	2.27	2.73	48.89	0.88	1.39
NSF ORCAS	40.24	39.17	1.07	4.05	35.12	0.39	0.68
All Campaigns	730.57	568.96	161.61	61.29	507.65	51.88	109.73

15 **Table S2.** The measurement range (minimum; maximum) of several key variables for individual campaigns restricted to cirrus cloud temperatures ≤ -40 °C.

Campaign	T (°C)	P (hPa)	RHi (%)	IWC (g/m ³)	Ni (#/L)	Di (μ m)	Na ₅₀₀ (#/cm ³)	Na ₁₀₀ (#/cm ³)
ATTREX	-88.1; -40	68.1; 330.5	1.65; 206.1	4.41×10^{-8} ; 0.443	0.037; 2.14×10^4	2.25; 401.32	-	-
POSIDON	-87.8; -40	63.1; 252.9	5.50; 212.4	7.68×10^{-8} ; 1.61	0.041; 2.26×10^4	2.25; 1510	-	-
SEAC ⁴ RS	-59.5; -40	178.7; 289.8	2.06; 156.7	4.86×10^{-8} ; 3.30	0.010; 3.10×10^4	2.10; 1455	0; 69.3	0; 688.4
NASA-DC3	-63.5; -40	178.2; 297.5	1.54; 161.8	3.19×10^{-6} ; 3.68	0.009; 1.70×10^5	20.0; 2500	0; 61.0	0; 3.55×10^3
MACPEX	-77.5; -40	74.1; 347.1	1.80; 161.8	2.73×10^{-6} ; 0.528	0.019; 1.95×10^3	20.0; 2105	0; 449.0	0; 2.10×10^3
CONTRAST	-78.3; -40	126.6; 331.3	0.378; 177.3	1.27×10^{-7} ; 1.02	0.042; 7.05×10^3	2.50; 1575	0; 6.86	0; 2.91×10^3
NSF-DC3	-65.8; -40	146.7; 321.9	1.24; 161.2	1.22×10^{-7} ; 1.44	0.046; 1.81×10^5	2.50; 2150	0; 15.2	0; 1.53×10^3
HIPPO	-77.2; -40	132.8; 531.3	0.482; 174.9	1.27×10^{-7} ; 0.930	0.042; 1.61×10^4	2.50; 2950	0; 712.2	0; 7.88×10^3
ORCAS	-68.8; -40	176.3; 433.2	0.334; 171.7	1.08×10^{-7} ; 0.243	0.043; 5.22×10^3	2.50; 975	0; 60.5	0; 537.2
PREDICT	-71.4; -40	140.3; 273.3	0.635; 191.7	1.27×10^{-7} ; 1.58	0.043; 4.06×10^4	2.50; 2850	0; 84.5	0; 568.6
START08	-67.6; -40	132.8; 447.3	0.331; 143.4	1.27×10^{-7} ; 1.68	0.042; 6.08×10^3	2.50; 1600	-	-
TORERO	-74.9; -40	123.8; 345.3	0.665; 149.6	4.29×10^{-8} ; 0.521	0.046; 1.37×10^3	2.50; 2200	0; 6.07	0; 274.13

Table S3. Linear regressions for analysis of aerosol-cloud interactions (ACI) in Figure 6 in the main manuscript. Intercept and

20 slope, and their standard deviations are shown as a , b , σ_a , and σ_b , respectively. IWC, Ni, and Di represent ice water content, ice crystal number concentrations, and number-weighted mean diameters, respectively.

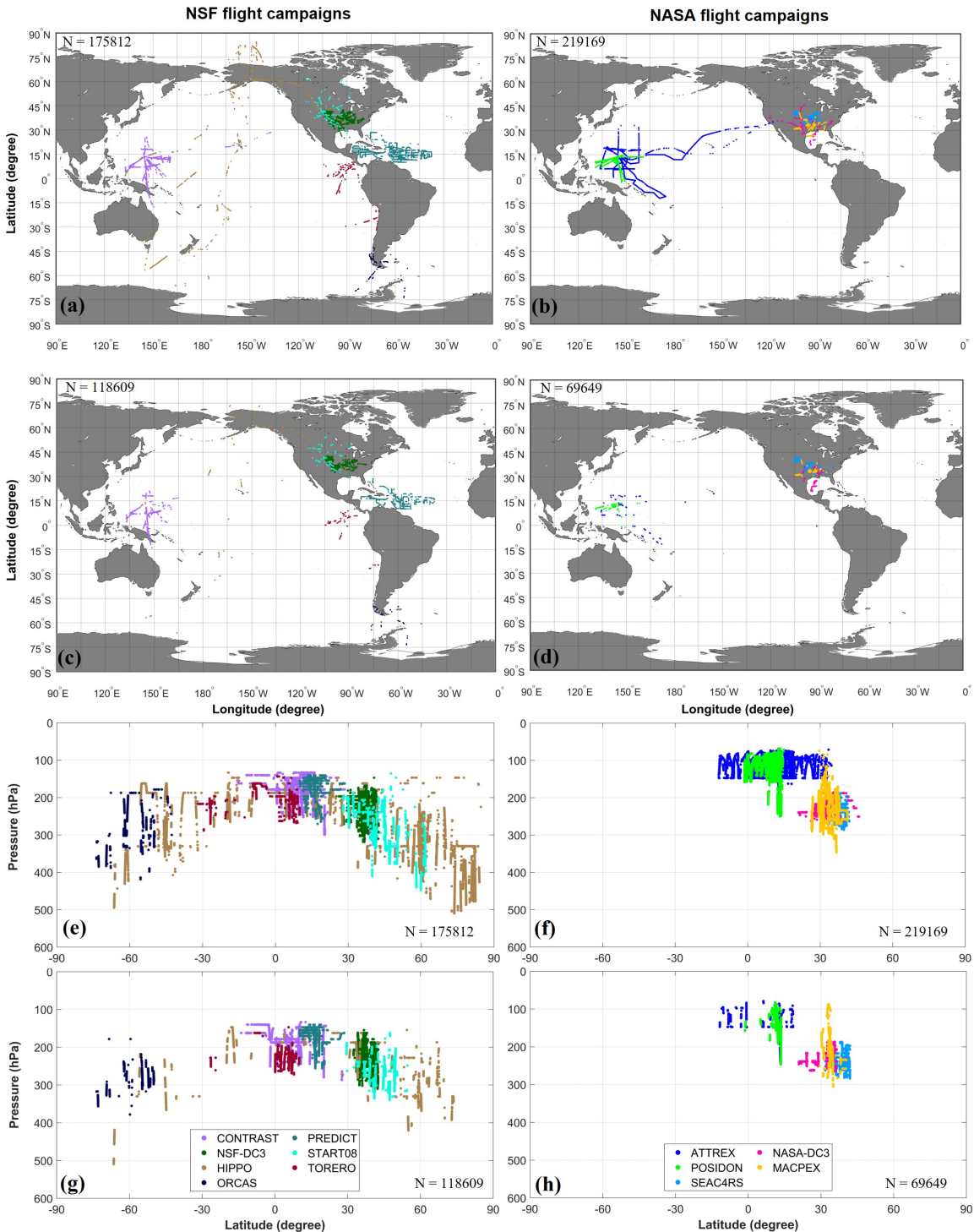
AIE at various temperature ranges													
	dlog ₁₀ (IWC)				dlog ₁₀ (Ni)				dlog ₁₀ (Di)				
Range (°C)	a	σ_a	b	σ_b	a	σ_a	b	σ_b	a	σ_a	b	σ_b	
dlog ₁₀ (Na ₅₀₀)	T ≤ -40	-0.126	0.049	1.155	0.043	-0.109	0.044	0.696	0.038	0.008	0.016	0.169	0.014
	-50 < T ≤ -40	-0.051	0.040	1.053	0.035	-0.006	0.053	0.651	0.046	-0.019	0.023	0.168	0.020
	-60 < T ≤ -50	-0.140	0.042	1.322	0.039	-0.087	0.047	0.714	0.044	0	0.013	0.201	0.012
	-70 < T ≤ -60	-0.286	0.078	1.477	0.079	-0.350	0.087	0.836	0.088	0.057	0.022	0.198	0.022
	-80 < T ≤ -70	0.160	0.165	3.674	0.557	0.061	0.115	1.675	0.388	0.028	0.002	0.518	0.006
dlog ₁₀ (Na ₁₀₀)	T ≤ -40	0.510	0.081	0.549	0.062	0.234	0.049	0.275	0.037	0.096	0.026	0.097	0.020
	-50 < T ≤ -40	0.346	0.118	0.632	0.097	0.306	0.052	0.387	0.043	0.008	0.034	0.078	0.028
	-60 < T ≤ -50	0.460	0.091	0.604	0.071	0.144	0.046	0.270	0.035	0.117	0.031	0.116	0.024
	-70 < T ≤ -60	0.416	0.094	0.658	0.083	0.123	0.033	0.064	0.029	0.100	0.029	0.233	0.026
	-80 < T ≤ -70	-0.172	0.083	-0.129	0.159	-0.081	0.055	-0.397	0.105	-0.028	0.024	0.098	0.046
AIE at various dRHi ranges													
	dlog ₁₀ (IWC)				dlog ₁₀ (Ni)				dlog ₁₀ (Di)				
Range (%)	a	σ_a	b	σ_b	a	σ_a	b	σ_b	a	σ_a	b	σ_b	
dlog ₁₀ (Na ₅₀₀)	dRHi ≤ -10	-0.359	0.045	1.172	0.040	-0.214	0.042	0.620	0.037	-0.024	0.017	0.207	0.015
	-10 < dRHi ≤ 0	-0.050	0.041	1.227	0.042	-0.054	0.070	0.853	0.070	0.003	0.020	0.125	0.020
	0 < dRHi ≤ 10	-0.023	0.054	1.120	0.056	-0.069	0.065	0.701	0.066	0.025	0.016	0.156	0.016
	dRHi > 10	0.018	0.063	1.182	0.071	-0.163	0.051	0.825	0.058	0.072	0.017	0.121	0.019
dlog ₁₀ (Na ₁₀₀)	dRHi ≤ -10	-0.375	0.121	0.759	0.107	-0.032	0.064	0.520	0.056	-0.099	0.030	0.080	0.027
	-10 < dRHi ≤ 0	0.380	0.076	0.699	0.061	0.242	0.057	0.302	0.045	0.045	0.026	0.141	0.021
	0 < dRHi ≤ 10	0.650	0.069	0.567	0.053	0.319	0.049	0.271	0.037	0.110	0.029	0.105	0.023
	dRHi > 10	0.691	0.069	0.350	0.055	0.233	0.047	0.228	0.038	0.157	0.013	0.041	0.011
AIE at various dw ranges													
	dlog ₁₀ (IWC)				dlog ₁₀ (Ni)				dlog ₁₀ (Di)				
Range (m/s)	a	σ_a	b	σ_b	a	σ_a	b	σ_b	a	σ_a	b	σ_b	
dlog ₁₀ (Na ₅₀₀)	dw ≤ -0.5	-0.149	0.065	1.387	0.072	0.050	0.035	0.974	0.039	-0.077	0.019	0.113	0.021
	-0.5 < dw ≤ 0	-0.169	0.054	1.198	0.047	-0.108	0.047	0.699	0.041	0	0.016	0.184	0.014
	0 < dw ≤ 0.5	-0.057	0.043	1.140	0.039	-0.074	0.042	0.673	0.038	0.016	0.019	0.173	0.017
	dw > 0.5	0.025	0.051	1.148	0.054	0.060	0.054	0.643	0.058	-0.024	0.015	0.187	0.016
dlog ₁₀ (Na ₁₀₀)	dw ≤ -0.5	0.502	0.108	0.381	0.095	0.409	0.071	0.423	0.062	0.006	0.023	-0.020	0.020
	-0.5 < dw ≤ 0	0.226	0.087	0.624	0.073	0.154	0.051	0.398	0.043	0.025	0.022	0.081	0.019
	0 < dw ≤ 0.5	0.517	0.079	0.513	0.065	0.217	0.046	0.297	0.037	0.109	0.022	0.075	0.018
	dw > 0.5	0.785	0.076	0.475	0.058	0.394	0.049	0.217	0.037	0.122	0.026	0.094	0.020

Table S4. Similar to Table 2 in Test A, but instead of excluding ATTREX, POSIDON, and START08 campaigns due to the lack of aerosol measurements, this Table S4 uses all NASA and NSF campaigns for ML experiments involved with predictors of T, RHi, and w . Accuracies of the cirrus occurrence predictions are shown for all cirrus, vertically quiescent, and non-quiescent cirrus in columns 1 – 3, respectively.

<i>Predictors</i>	<i>Accuracy (%)</i>	<i>Accuracy (%)</i>	<i>Accuracy (%)</i>
	<i>All cirrus</i>	<i>Vertically quiescent cirrus</i>	<i>Non-quiescent cirrus</i>
<i>1 Predictor</i>			
<i>T</i>	57.30	57.69	55.32
<i>RHi</i>	85.30	85.01	86.79
<i>w</i>	68.04	71.39	50.79
<i>2 Predictors</i>			
<i>T + RHi</i>	86.53	86.41	87.16
<i>T + w</i>	64.18	66.39	52.80
<i>RHi + w</i>	85.41	85.16	86.73
<i>3 Predictors</i>			
<i>T + RHi + w</i>	86.58	86.46	87.20

Table S5. Similar to Table 2, but using water vapor mixing ratio “q” (unit: ppmv) instead of RHi as a predictor variable.

Predictors	Accuracy (%)	Accuracy (%)	Accuracy (%)
	All cirrus	Vertically quiescent cirrus	Non-quiescent cirrus
<i>1 Predictor</i>			
<i>T</i>	63.46	65.65	54.26
<i>q</i>	76.38	76.41	76.25
<i>w</i>	71.04	75.96	50.37
<i>Na₅₀₀</i>	84.32	88.96	64.83
<i>Na₁₀₀</i>	68.94	70.27	63.33
<i>2 Predictors</i>			
<i>T + q</i>	90.59	90.89	89.35
<i>T + w</i>	73.23	78.02	53.07
<i>T + Na₅₀₀</i>	73.18	76.18	60.55
<i>T + Na₁₀₀</i>	68.70	69.98	63.30
<i>q + w</i>	76.40	76.46	76.12
<i>q + Na₅₀₀</i>	77.23	77.02	78.13
<i>q + Na₁₀₀</i>	79.83	80.31	77.82
<i>w + Na₅₀₀</i>	76.17	81.42	54.11
<i>w + Na₁₀₀</i>	70.78	73.85	57.87
<i>Na₅₀₀ + Na₁₀₀</i>	72.63	74.24	65.86
<i>3 Predictors</i>			
<i>T + q + w</i>	90.31	90.63	88.99
<i>T + q + Na₅₀₀</i>	90.76	91.12	89.23
<i>T + q + Na₁₀₀</i>	90.92	91.33	89.18
<i>T + w + Na₅₀₀</i>	77.50	82.51	56.45
<i>T + w + Na₁₀₀</i>	74.23	77.10	62.18
<i>T + Na₅₀₀ + Na₁₀₀</i>	71.55	73.49	63.40
<i>q + Na₅₀₀ + Na₁₀₀</i>	80.47	80.85	78.89
<i>q + w + Na₅₀₀</i>	77.17	76.93	78.19
<i>q + w + Na₁₀₀</i>	80.04	80.27	79.07
<i>w + Na₅₀₀ + Na₁₀₀</i>	74.83	78.51	59.37
<i>4 Predictors</i>			
<i>T + q + w + Na₅₀₀</i>	90.47	90.79	89.12
<i>T + q + w + Na₁₀₀</i>	90.52	90.90	88.96
<i>T + q + Na₅₀₀ + Na₁₀₀</i>	90.90	91.33	89.09
<i>T + w + Na₅₀₀ + Na₁₀₀</i>	76.66	79.84	63.27
<i>q + w + Na₅₀₀ + Na₁₀₀</i>	80.94	81.07	80.40
<i>5 Predictors</i>			
<i>T + q + w + Na₅₀₀ + Na₁₀₀</i>	90.58	90.97	88.98



30

Figure S1. Global maps and vertical profiles of cirrus cloud measurements at temperatures ≤ -40 °C based on seven NSF (left) and five NASA (right) flight campaigns. (a, b, e, f) Vertically quiescent cirrus clouds. (c, d, g, h) Non-quiescent cirrus clouds.

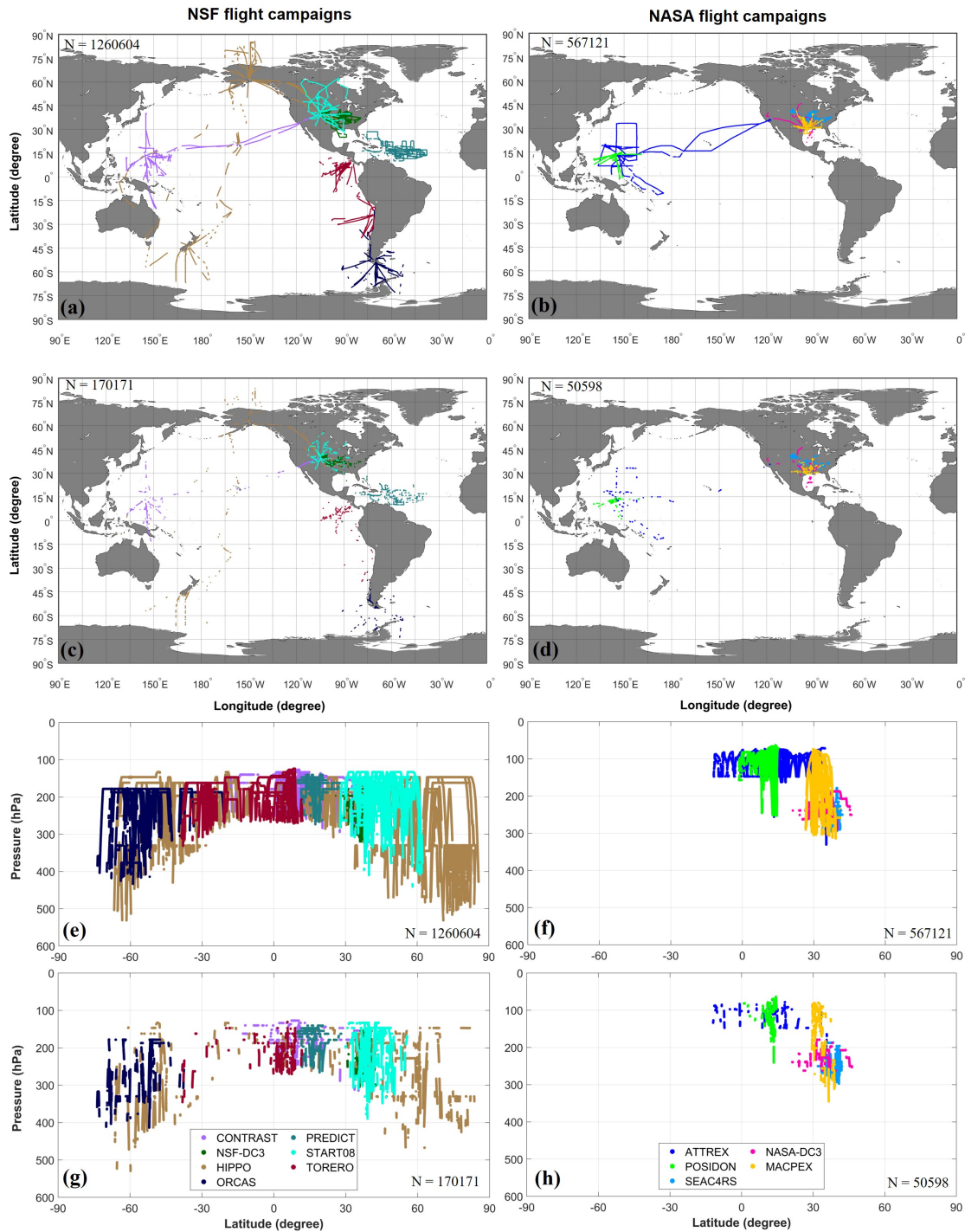
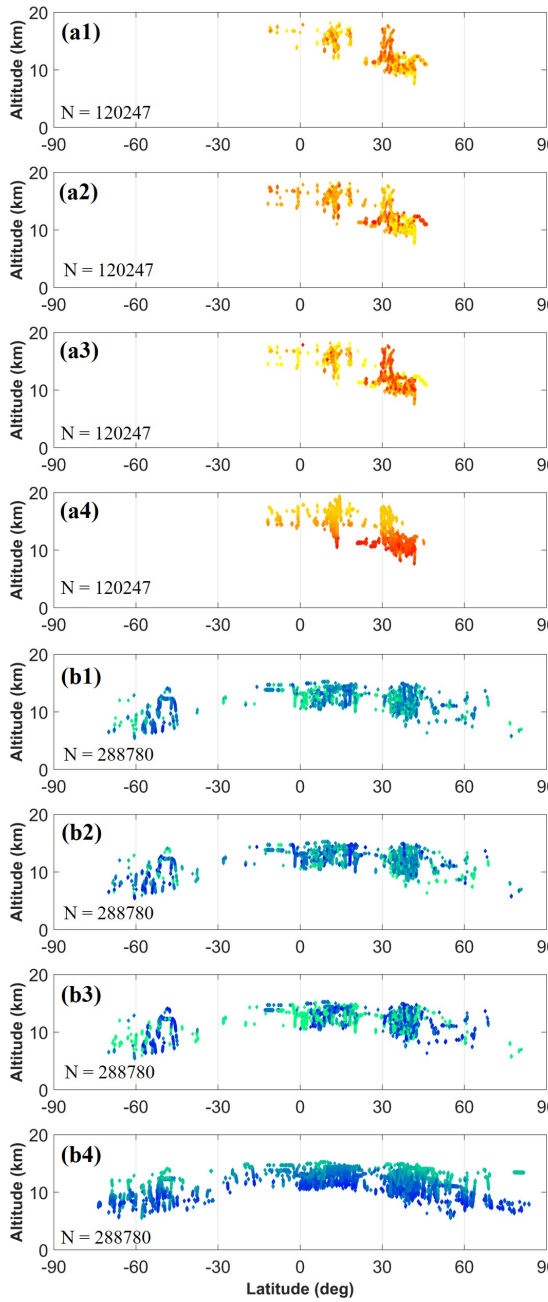


Figure S2. Similar to Figure S1, but for clear-sky samples in (a, b, e, f) vertically quiescent and (c, d, g, h) non-quiescent

35 conditions.

Non-quiescent conditions



Vertically quiescent conditions

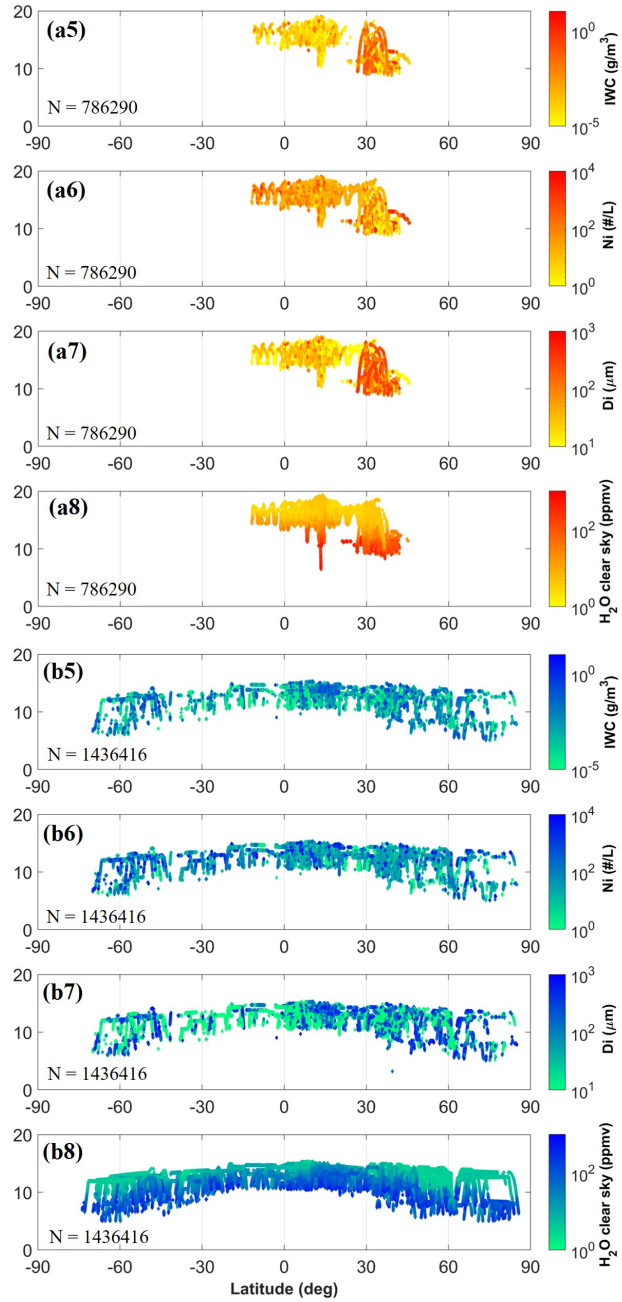
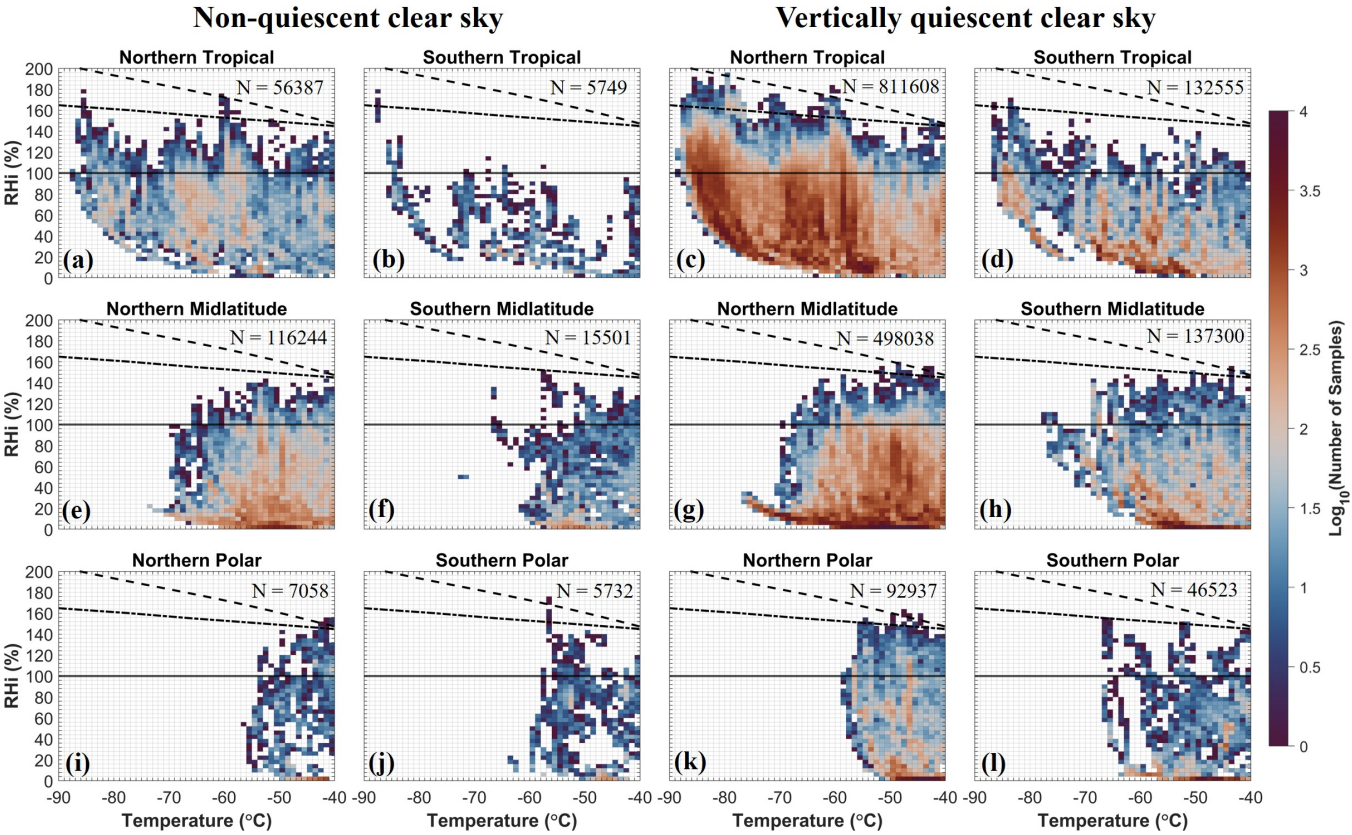
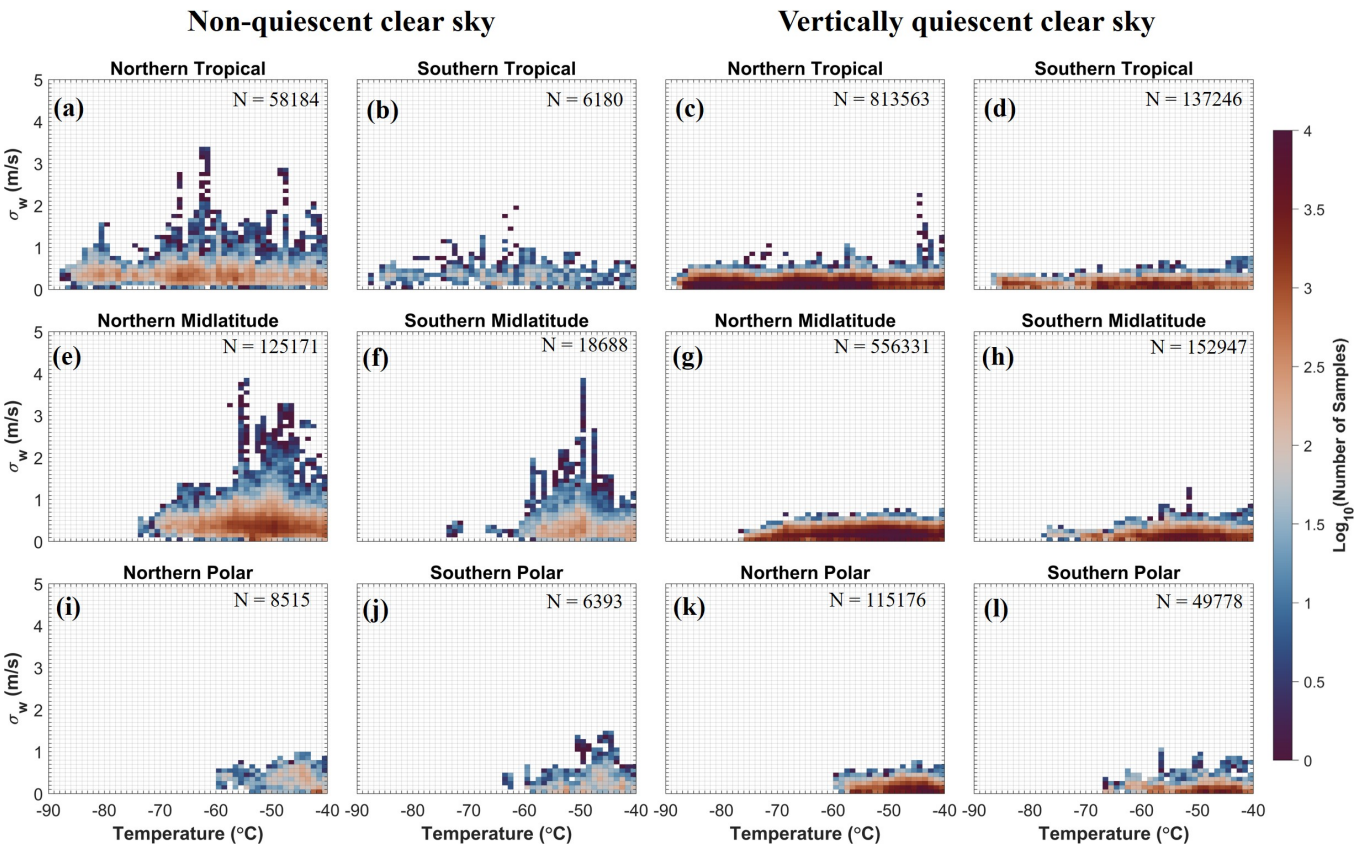


Figure S3. Vertical distributions of IWC, Ni, Di, and clear-sky water vapor volume mixing ratio for temperatures $\leq -40^\circ\text{C}$ during the research flights in (a1-a8) NASA and (b1-b8) NSF campaigns. Observations are additionally separated by non-quiescent (left) and vertically quiescent conditions (right).



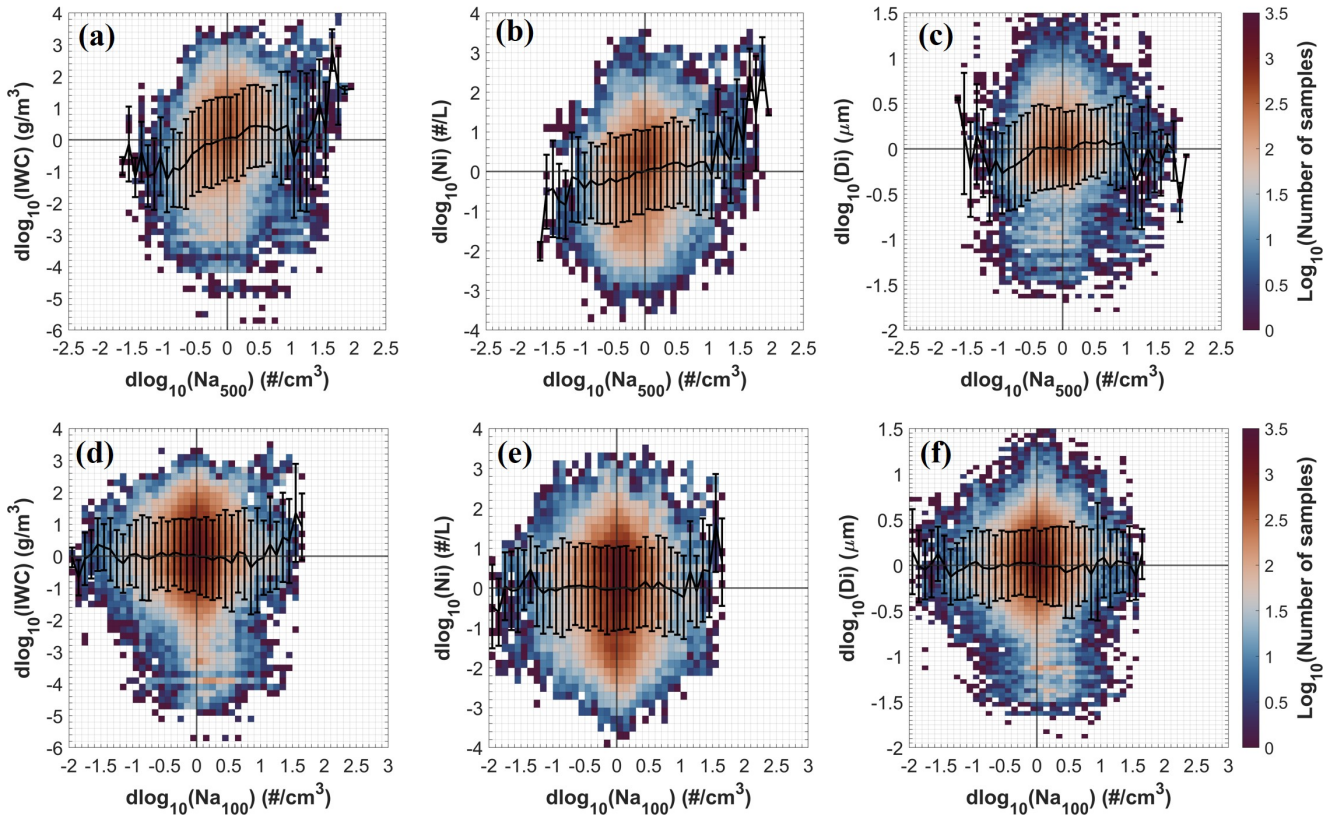
40

Figure S4. Similar to Figure 2 in the main manuscript, but for distributions of clear-sky RHi as a function of temperature associated with non-quiescent (left two columns) and vertically quiescent conditions (right two columns).



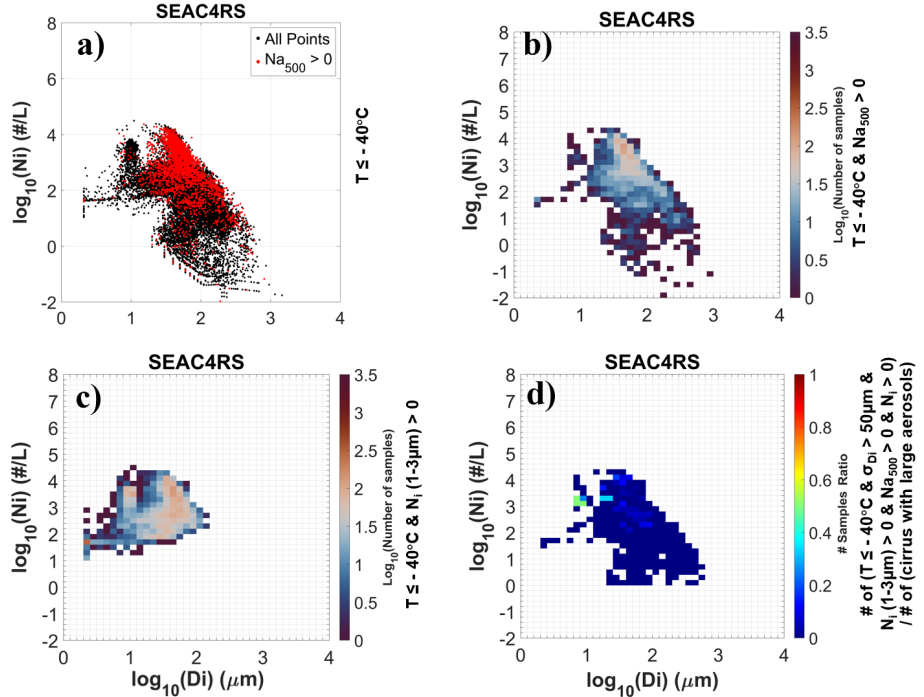
45 **Figure S5.** Similar to Figure 3 in the main manuscript, distributions of standard deviations of vertical velocity (σ_w , calculated for 10 km spatial scales) for clear-sky conditions that are Non-quiescent (left two columns) and vertically quiescent (right two columns).

NASA + NSF (1 – 3012.5 μm) (clear-sky Na)



50

Figure S6. Similar to Figure 5, except for the analysis of clear-sky Na instead of in-cloud Na. Distributions of IWC, Ni, and Di with respect to (a-c) Na_{500} and (d-f) Na_{100} using the clear-sky Na values calculated at 100-s scale. Black lines and vertical bars denote the geometric means and standard deviations, respectively.



55

60

Figure S7. Distributions of samples for the NASA SEAC⁴RS campaign. All panels are restricted to temperature $\leq -40^\circ\text{C}$. (a) Scatter plots of all cirrus samples in black as well as those with $\text{Na}_{500} > 0$ in red. (b) Number of samples for cirrus clouds with $\text{Na}_{500} > 0$. (c) Number of samples for cirrus clouds with small ice, i.e., $\text{Ni}_{1-3\mu\text{m}} > 0$, regardless of aerosol existence. (d) Ratio of number of samples of two conditions, i.e., samples with possible shattering indicators versus total cirrus samples with large aerosols.

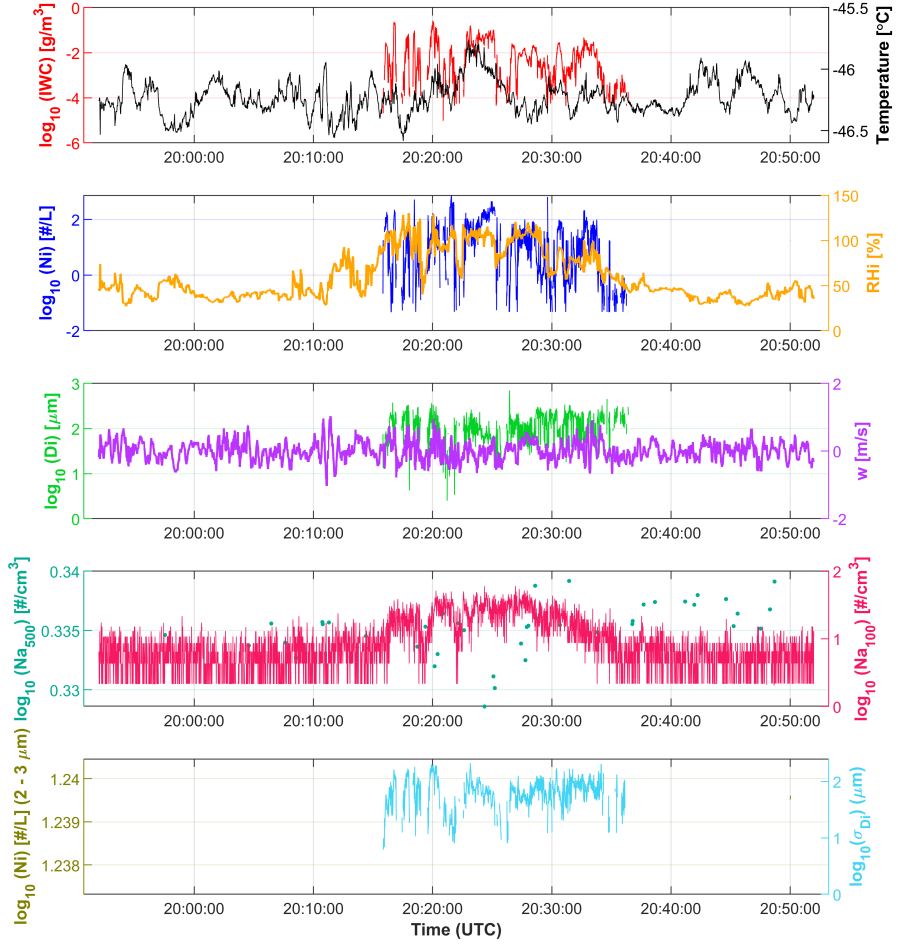


Figure S8. An example of time series from NSF DC3 RF20 on June 21, 2012. The Na_{500} values show a decreasing trend inside the cirrus segment at UTC 20:20 – 20:30 compared with the surrounding clear-sky conditions, while the Na_{100} values show an increasing trend for in-cloud segment. The Na_{500} samples also show much fewer data than the Na_{100} samples, indicating relatively fewer large aerosols at cirrus level.

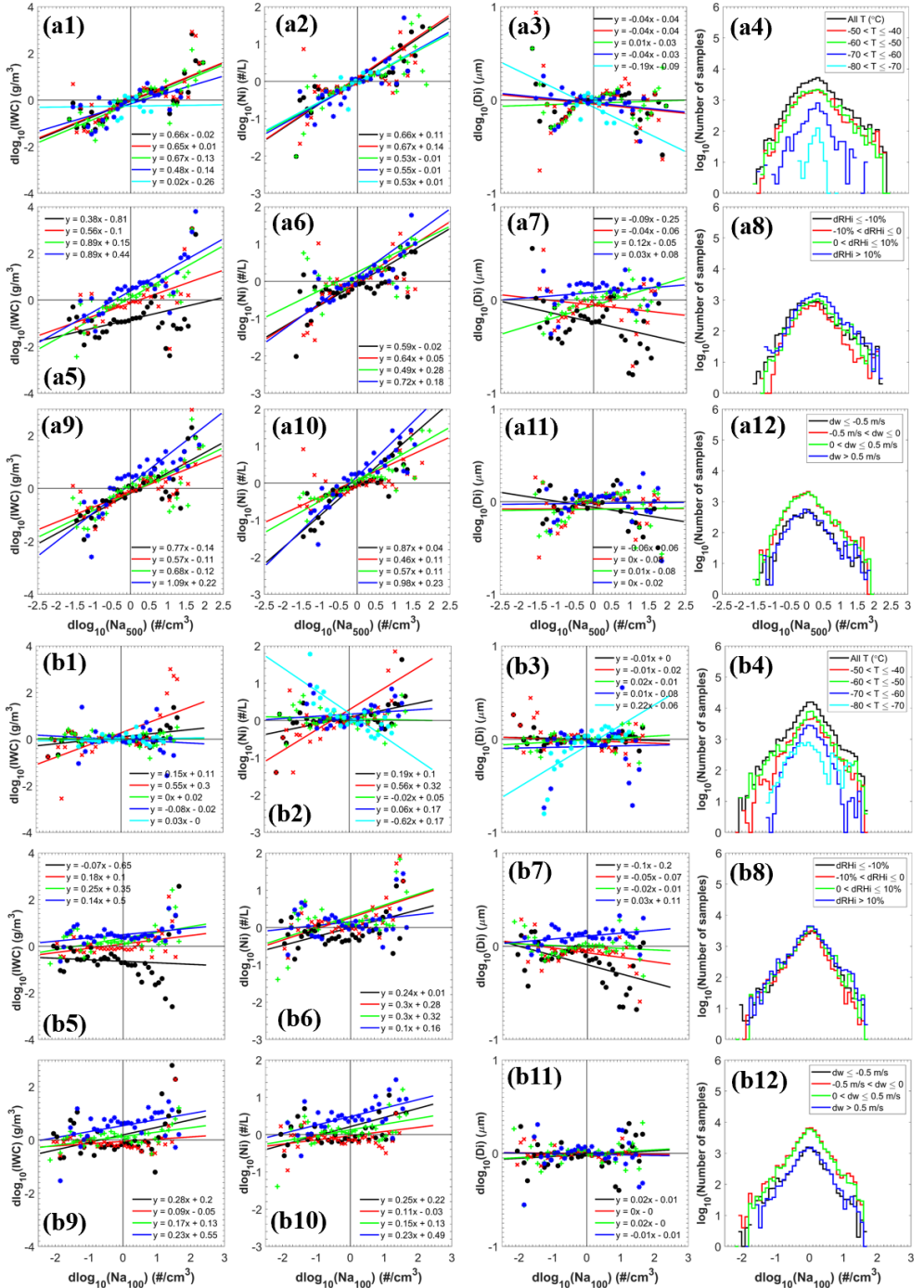


Figure S9. Similar to Figure 6 in the main manuscript, but using clear-sky Na values. ACI is examined for various ranges of temperature, dRHi, and dw. Colored dots represent geometric means of ice microphysical properties in each Na bin. Slope and intercept values are shown in the legend. The last column represents the number of samples.

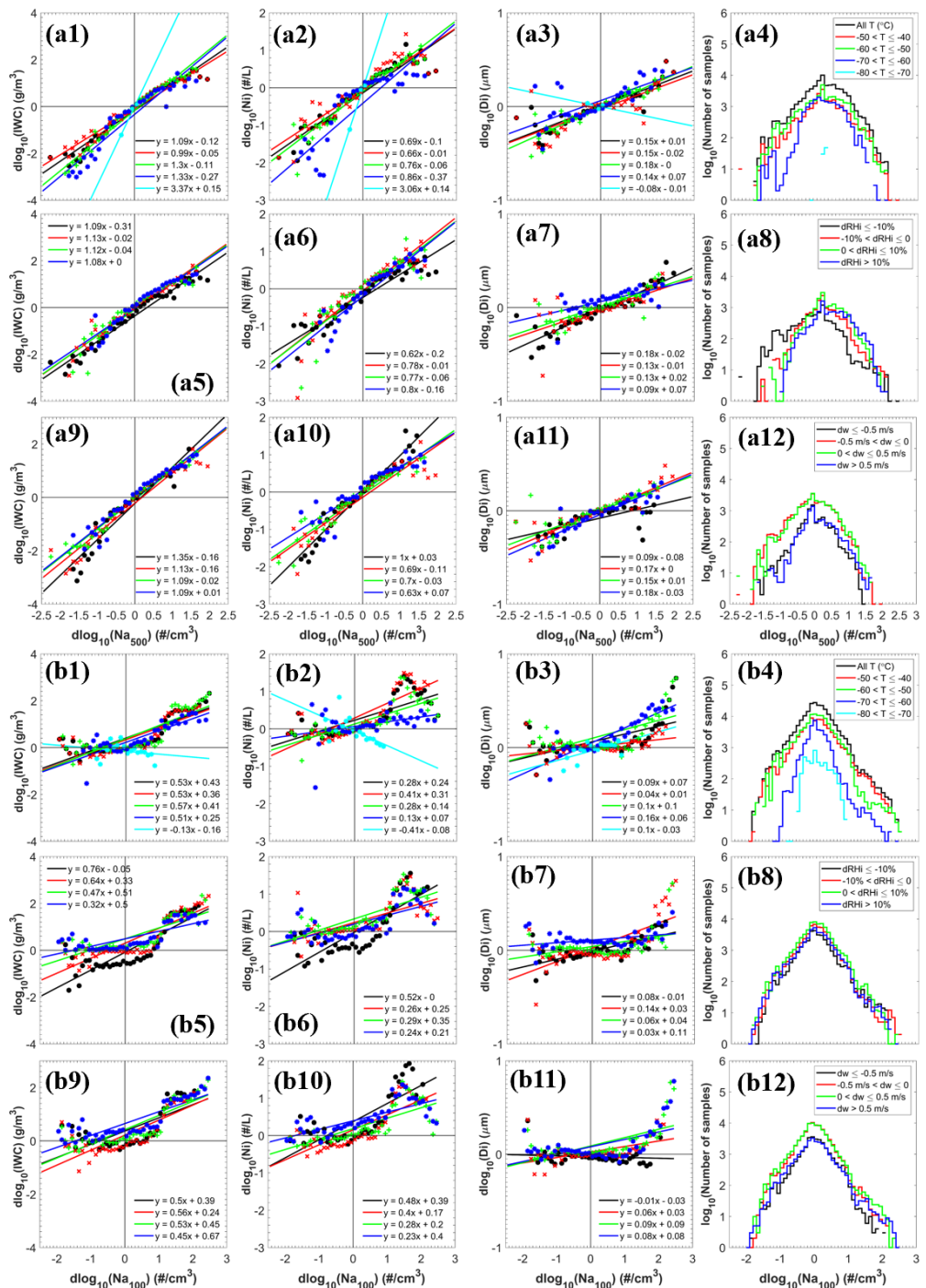
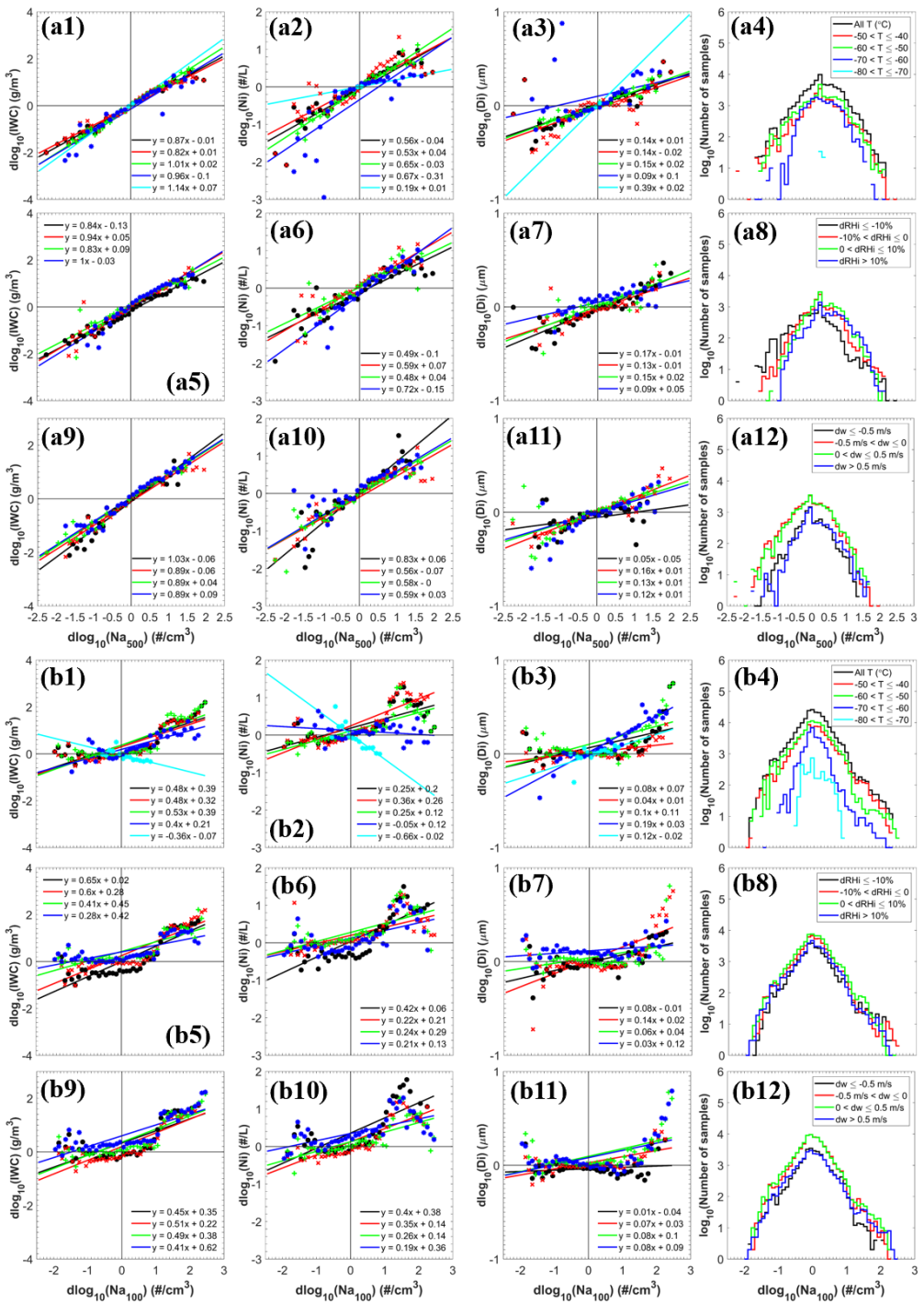


Figure S10. Similar to Figure 6 in the main manuscript, except for using a higher threshold for in-cloud definition, i.e., in-cloud conditions are defined as $\text{IWC} > 10^{-5} \text{ g m}^{-3}$.



75 **Figure S11.** Similar to Figure 6 in the main manuscript, except for using a higher threshold for in-cloud definition, i.e., in-cloud conditions are defined as IWC > 10⁻⁴ g m⁻³.

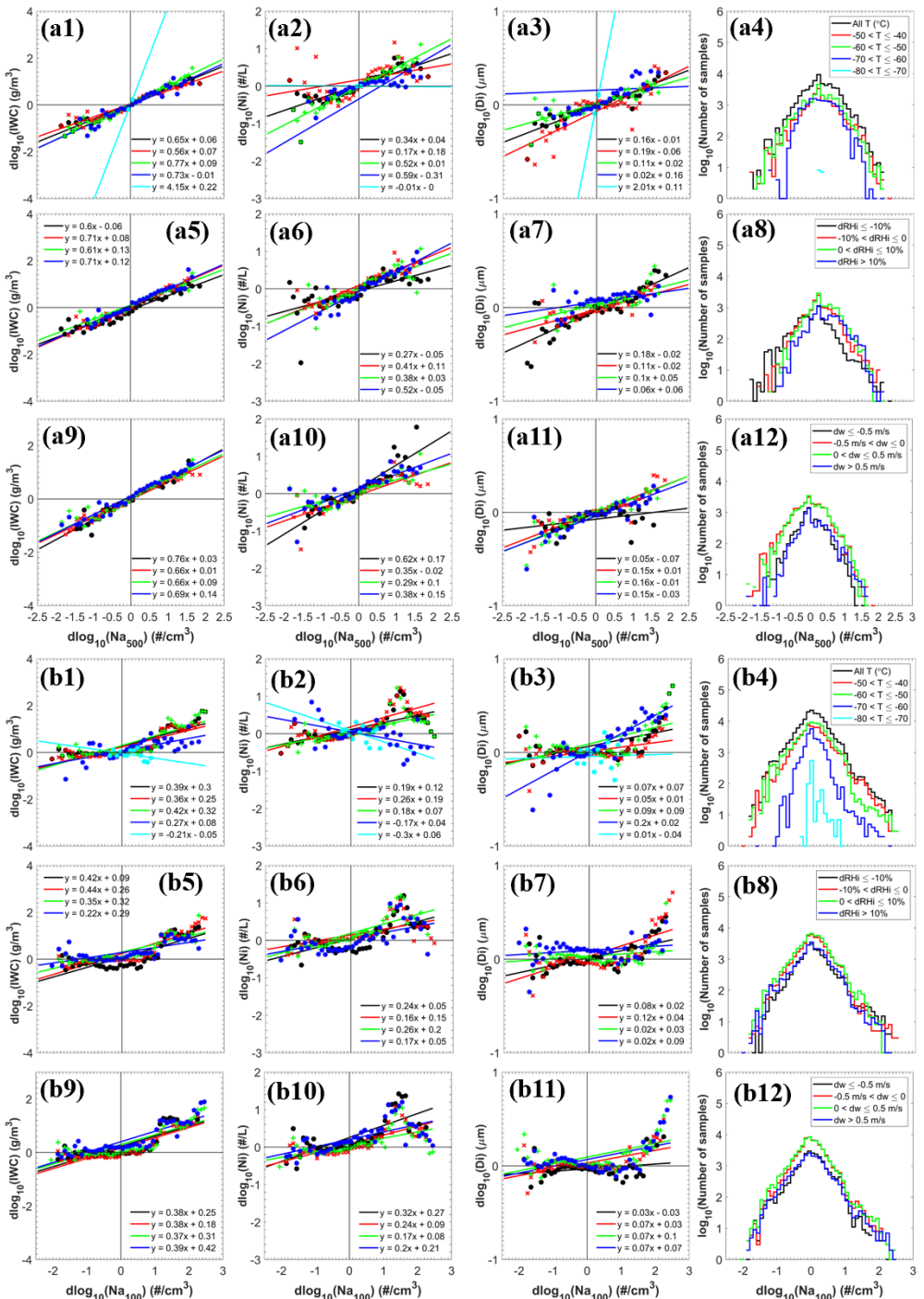


Figure S12. Similar to Figure 6 in the main manuscript, except for using a higher threshold for in-cloud definition, i.e., in-cloud conditions are defined as IWC > 10⁻³ g m⁻³.